IDEAL J. Mol. Biol. (1999) 287, 837–843

JMB

COMMUNICATION

X-ray Diffraction from a Single Layer of Purple Membrane at the Air/Water Interface

Stephan A. W. Verclas[1,2,5], Paul B. Howes[3], Kristian Kjaer[3] Angelika Wurlitzer[4], Markus Weygand[4], Georg Büldt[5] Norbert A. Dencher[1,2] and Mathias Lösche[4]*

[1]*Institute of Biochemistry Technische Universität Darmstadt, Petersenstr. 22 D-64287 Darmstadt, Germany*

[2]*Hahn-Meitner-Institut BENSC (NE/Biophysik), Glienicker Str. 100 D-14109 Berlin, Germany*

[3]*Physics Department Risø National Laboratory DK-4000 Roskilde, Denmark*

[4]*Institute of Experimental Physics I, Universität Leipzig Linnéstr. 5, D-04103 Leipzig Germany*

[5]*Institute for Structural Biology (IBI-2), Forschungszentrum Jülich, D-52415 Jülich Germany*

**Corresponding author*

X-ray diffraction patterns have been recorded from a single layer of purple membrane (~50 Å thickness) at the air/water interface in a Langmuir trough. Grazing-incidence X-ray diffraction is demonstrated to be a promising method for obtaining structural information on membrane proteins under physiological conditions. The method is so sensitive that diffraction can be measured from samples with only 10^{13} protein molecules in the beam. Diffraction from hexagonal crystals of purple membrane with a lattice constant of 61.3 Å was observed up to the order $\{h,k\} = \{4,3\}$, corresponding to a resolution of ~9 Å. The work reported here is a first step towards a new way of protein crystallography using grazing-incidence X-ray diffraction at the air/water interface.

Keywords: grazing-incidence X-ray diffraction; bacteriorhodopsin; purple membrane; protein crystallography; Langmuir films

The crystallography of proteins has revolutionized our understanding of biological processes. It has provided an understanding of function on the basis of structures at atomic resolution for a steadily growing number of biomolecules. The bottleneck is the formation of well-ordered three-dimensional (3D) crystals. Numerous important biological processes are mediated by integral membrane proteins. Unfortunately, membrane proteins are less amenable to 3D crystallization, and only a few structures of membrane proteins have been solved by X-ray crystallography. To circumvent this problem, electron crystallography was applied using two-dimensional (2D) protein crystals analyzed in vitrified ice or after heavy ion staining under ultra-high vacuum in the electron microscope (Henderson *et. al*., 1990; Uzgiris & Kornberg, 1983). A technical difficulty of this approach is the inaccessibility of scattered intensity near the *l*-axis of the reciprocal space (''hidden cone problem'').

Here, we use a different approach, applying crystallographic methods to a single protein layer on the surface of an aqueous subphase by means of grazing-incidence X-ray diffraction (GIXD). GIXD has been widely employed for the structural characterization of lipid monolayers (Als-Nielsen *et al*., 1994). However, its application to proteins has only recently been demonstrated in an investigation of the water-soluble protein streptavidin attached to a monolayer of lipids (Haas *et al*., 1995). An advantage of GIXD is its high degree of surface sensitivity which comes about because under total reflection of the incident beam, the

Abbreviations used: PM, purple membrane; BR, bacteriorhodopsin; GIXD, grazing-incidence X-ray diffraction; 3D, three-dimensional; 2D, two-dimensional; PSD, position-sensitive detector.

E-mail address of the corresponding author: loesche@physik.uni-leipzig.de

0022-2836/99/150837–07 $30.00/0

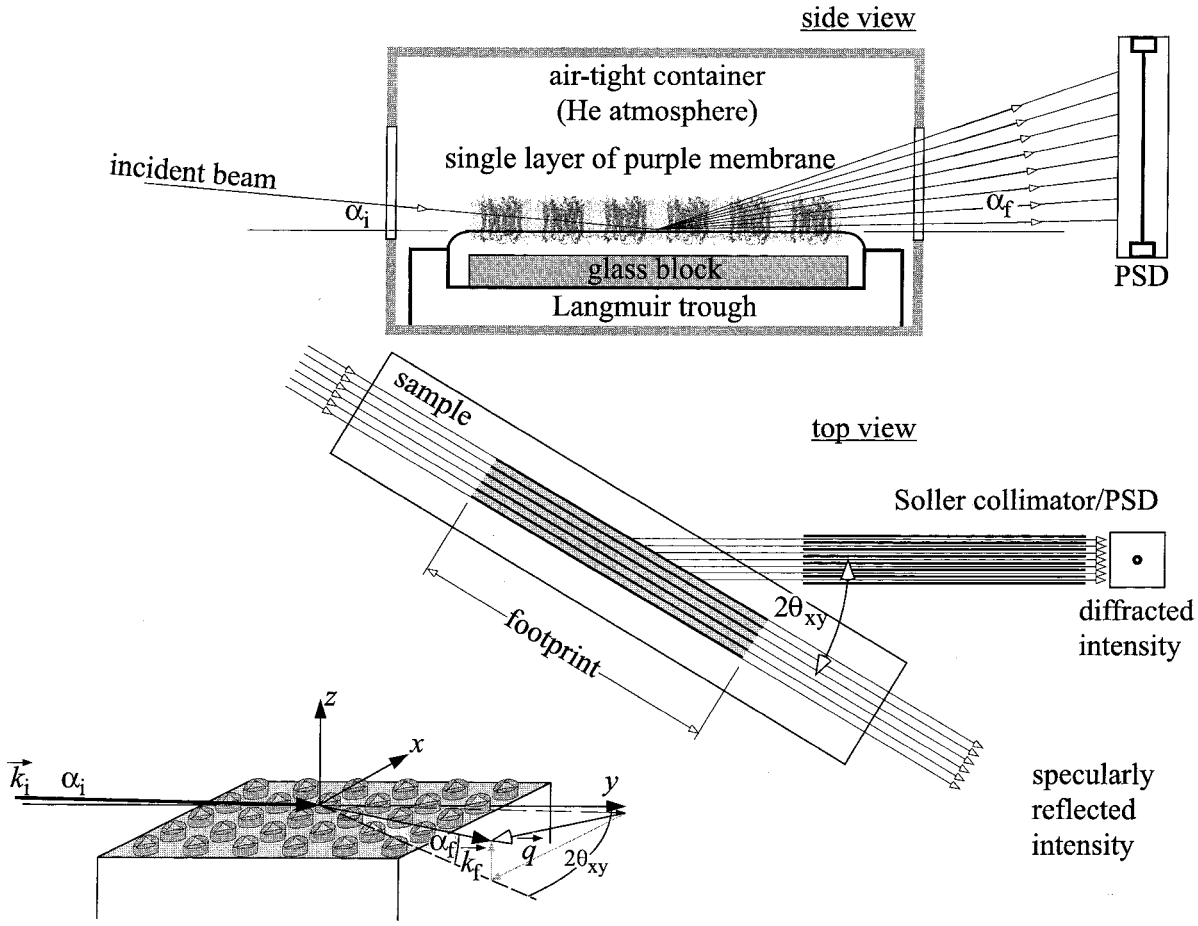

Figure 1. Schematic representation of the GIXD experiment. Top: side view showing the X-ray beam impinging upon a PM single layer film on the air/water interface. Center: top view of the experimental setup. Lower left: coordinate system and scattering vector.

evanescent wave penetrates less than 100 Å beneath the surface so that the bulk subphase is not illuminated (cf. Als-Nielsen & Kjaer, 1989; Als-Nielsen *et al.*, 1994). With a 2D powder of (typically) 10^{13} protein molecules, this allows detection of the faint diffraction signal which would otherwise have been swamped by background scattering from the liquid subphase. Furthermore, the technique can be applied under physiological conditions which reduces the liability to preparation artifacts (no stain or cryo-fixation needed, no inspection of the sample under ultra-high vacuum conditions).

We have tested this promising structural approach with bacteriorhodopsin (BR), the only protein in the purple membrane (PM) of *Halobacterium salinarum*. BR ($M_r \sim 27$ kDa) is the prototype of an integral membrane protein and functions as a light-driven proton pump (Oesterhelt & Stoeckenius, 1973). BR is one of the most promising candidates to elucidate the link between the structure of a membrane transport protein, its dynamics, and function. The structure of BR, its arrangement in the PM (Henderson *et al.*, 1990; Grigorieff *et al.*, 1996; Pebay-Peyroula *et al.*, 1997; Essen *et al.*, 1998) and the light-induced structural changes are sufficiently well known (Dencher *et al.*, 1989, 1991; Koch *et al.*, 1991) to serve as a test object to study the potential of GIXD for structure determination of membrane proteins. The method that we describe here has a broad application potential: instead of depositing a single layer of purple membrane at the air/water interface of a Langmuir trough, as in the present study, protein molecules can also be anchored to surfaces by various surface-modification protocols (Uzgiris & Kornberg, 1983; Ribi *et al.*, 1987; Darst *et al.*, 1991; Hirata & Miyake, 1994; Pack *et al.*, 1997; Schmitt & Tampé, 1996; Dietrich *et al.*, 1996).

Purple membrane was isolated from *H. salinarum* and purified as described by Bauer *et al.* (1976). In addition to native PM with a lipid content of ~25% wt, we have also used delipidated PM (Glaeser *et al.*, 1985; Fitter *et al.*, 1996) with only 5% lipids. Lipids were partially removed from PM without solubilization of BR by treatment with CHAPS (3-[(3-cholamidopropyl)dimethylammonio]-1-propanesulphonate; Boehringer Mannheim) as described by Fitter *et al.* (1996). PM patches were deposited in a single-layer film at the air/water interface. Film formation was optimized beforehand by means of fluorescence microscopy

(Lösche & Möhwald, 1984; Krüger *et al.*, 1999) using PM labeled with fluorescein at the extracellular surface of BR (Dencher *et al.*, 1991). The PM film was deposited on the aqueous surface in a Langmuir film balance *via* a wet glass slide touching the surface at an oblique angle. Typically, 1 ml of a PM suspension (120 μg BR/ml) was delivered in small droplets on the glass slide. It flowed to the surface of the saline solution where it was observed to increase the lateral pressure, Π (equivalent to a reduction of the surface tension). For further characterization, floating films of PM patches were transferred at various lateral pressures from the aqueous surface to glass slides by the horizontal dipping technique, and examined in an atomic force microscope (DI Nanoscope E). In such experiments, we invariably observed patches of 300 to 500 nm in diameter with a homogeneous height of 50 to 60 Å. The number of patches per unit area increased with increasing Π, and for $\Pi \geqslant 25$ mN/m the patches were frequently observed to overlap. Whether this overlap reflects the true structure on the water surface or occurred upon transfer to glass slides has not been investigated.

GIXD experiments were performed at the undulator beamline BW1 of HASYLAB (DESY, Hamburg) on the liquid surface diffractometer (cf. Weissbuch *et al.*, 1997; Weygand *et al.*, 1999). A Langmuir trough is placed in a sealed container under a humidified helium atmosphere to reduce background scattering. The area of the water surface in the trough is 440 cm^2. A wavelength $\lambda \sim 1.45$ Å (1.448 Å or 1.456 Å in different runs) was obtained by reflection from a Beryllium (002) monochromator crystal. The X-ray beam was adjusted to impinge on the surface at an incidence angle of $\alpha_i \sim 0.85 \cdot \alpha_c$ (cf. Figure 1, top), where $\alpha_c \sim 0.14^\circ$ is the critical angle for total reflection from water. The diffracted radiation was collected by a one-dimensional position-sensitive detector (PSD) oriented vertically and scanned by varying the horizontal scattering angle, $2\theta_{xy}$. The area of the footprint (Figure 1, center) of the incoming X-ray beam on the liquid surface was adjusted to 1 mm × 50 mm at small $2\theta_{xy}$ and to 3 mm × 50 mm at larger $2\theta_{xy}$. The lowest accessible $2\theta_{xy}$ ($\sim 1^\circ$) is well below the $\{h,k\} = \{1,0\}$ Bragg reflection of the BR lattice, which could thus be resolved at $q_{xy} \sim (4\pi/\lambda) \cdot \sin(2\theta_{xy}/2) = 0.12$ $Å^{-1}$, $2\theta_{xy} = 1.63^\circ$. (For a definition of the coordinate system, see Figure 1, lower left). Data were collected up to $2\theta_{xy} = 10^\circ$, such that the intense {4,3} Bragg reflection at $2\theta_{xy} \sim 9.6^\circ$ ($q_{xy} \sim 0.72$ $Å^{-1}$) could be observed. The Bragg rods, i.e., the intensity distribution above the horizon, were measured between $\alpha_f = 0$ and 9° ($q_z \approx (2\pi/\lambda)\sin(\alpha_f)$ = 0 and 0.677 $Å^{-1}$).

Generally, crystallites in the film on the water surface are of micrometer size (see below) and are randomly oriented around the vertical axis so that the film is a 2D powder.

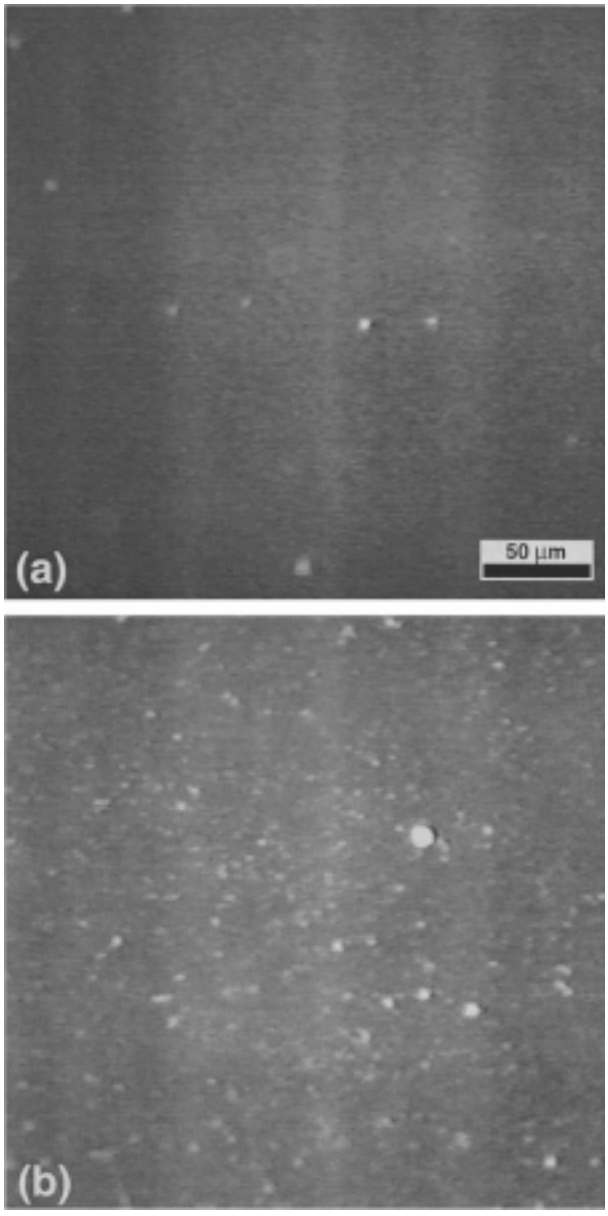

Figure 2. Fluorescence micrographs of a PM monolayer with fluorescein-labeled BR on an aqueous subphase containing 200 mM KCl. (a) Immediately after spreading, $\Pi = 0$ mN/m; (b) after compression to $\Pi = 10$ mN/m.

Fluorescence microscopy

The preparation protocol for protein/lipid single surface layers was optimized by observing PM patches with fluorescein-labeled BR using fluorescence microscopy. After spreading, the surface film at $\Pi \sim 0$ mN/m is rather inhomogeneous and consists of areas with a large density of the fluorescent patches coexisting with areas showing low patch density. Figure 2(a) depicts such a low-density area at $\Pi \sim 0$ mN/m, $T \sim 20\,^\circ$C, immediately after spreading the sample. There are a few small fluorescent dots which presumably represent single PM patches. Note that the fluorescent dots may

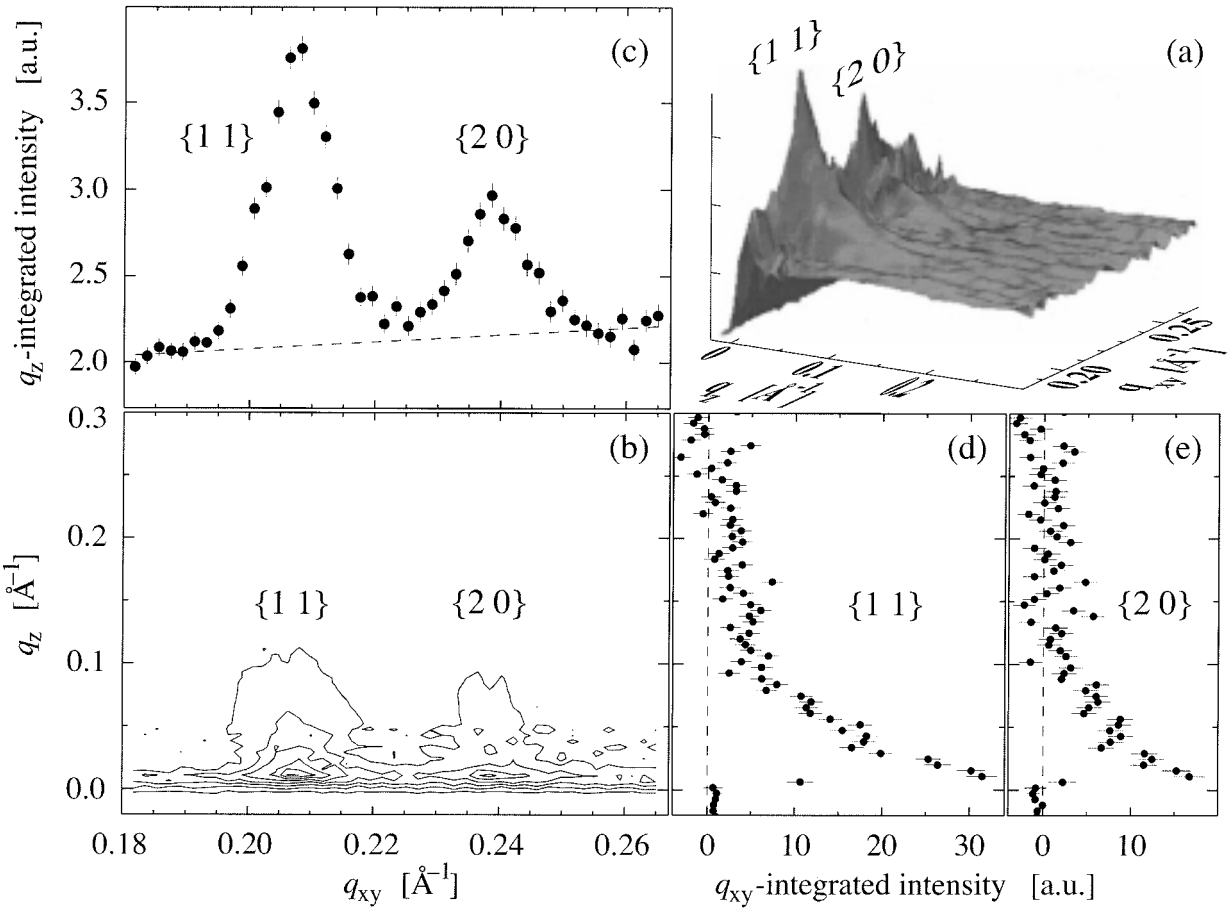

Figure 3. Grazing-incidence X-ray diffraction from patches of purple membrane at the air/solution interface at $\Pi = 5$ mN/m on a subphase containing 200 mM KCl. Close-up showing the {11} and {20} peaks. (a) Surface plot and (b) contour plot showing the scattered intensity as function both of the horizontal component, q_{xy}, and of the vertical component, q_z, of the scattering vector. Note that all the diffracted intensity (above background) is concentrated near the horizon ($0 < q_z < 0.1$ Å^{-1}). Below the horizon ($q_z < 0$), no intensity is observed, and just above the horizon ($q_z \sim 0.01$ Å^{-1}) the intensity pattern is modulated by a sharp maximum. This so-called Vineyard peak is due to constructive interference between X-rays diffracted upward and X-rays diffracted downwards to negative q_z and subsequently total-reflected back up by the interface (Vineyard, 1982; Als-Nielsen & Kjaer, 1989; Kjaer, 1994). (c) Projection of (b) on the horizontal axis, showing intensity *versus* q_{xy}. Two Bragg peaks, {11} and {20}, of the 2D powder pattern are seen. The broken line is the estimated background. (d), (e) Projection of (b) on the vertical axis; after background subtraction, the intensity was integrated over q_{xy} for each of the two peaks yielding the {11} and {20} Bragg rod intensities *versus* q_z.

appear larger than they are due to the large contrast between the non-fluorescent background and the labeled patches. Figure 2(b) shows the same film at the interface after compression to $\Pi \sim 10$ mN/m. The whole field of view in the through is covered with PM. To allow PM interface films to form on the water surface, PM was spread on a 200 mM KCl subphase. At lower ionic strength, PM was observed to gradually submerge into the subphase. In particular, it was impossible to obtain stable surface films on pure water, as also observed by Furuno *et al*. (1988).

GIXD

GIXD data from single layer PM films at the air/water interface have been collected between $q_{xy} \sim 0.08$ and 0.8 Å^{-1}. Since X-ray damage is a serious concern, we have measured the decay of the intensity diffracted into the $\{h,k\} = \{1,1\}$ reflection at $2\theta_{xy} \sim 2.75^\circ$ upon exposure and observed decay times of $\tau \sim 30$ minutes at typical currents in the storage ring (80 mA). Thus, to minimize radiation damage, during scans of $2\theta_{xy}$ the surface film was translated across the beam by moving the Langmuir film balance on a horizontal translation stage, such that the exposure of any area within the film was less than ten minutes. An intensity contour plot, I *versus* q_{xy} and q_z, of a PM surface film on 200 mM KCl at $\Pi = 5$ mN/m is shown in Figure 3. The low q_{xy} range that contains the {1,1} and {2,0} Bragg reflections of the hexagonal lattice is shown. The Bragg rod intensity is centered at the horizon ($q_z = 0$) and for $q_z > 0.2$ Å^{-1}, no scattered intensity is detected above the background. Figure 4 shows an extended data set for a sample

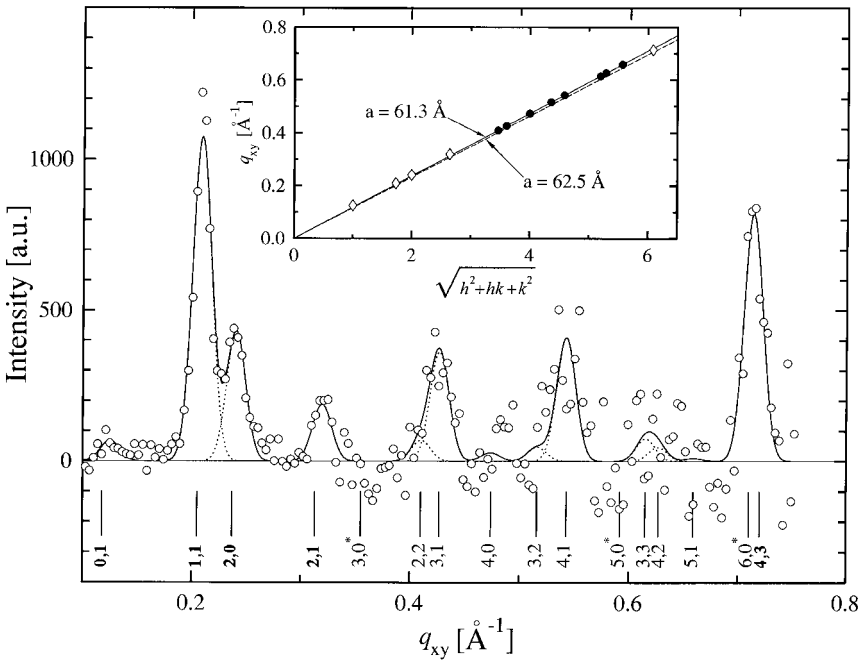

Figure 4. PM at $\Pi = 10$ mN/m on 250 mM KCl. Scattered intensity, normalized and corrected for angular factors, as a function of the horizontal component q_{xy} of the scattering vector. The signal was integrated over vertical exit angles, α_f, between 0° and 1.0° ($q_z = 0$ to 0.075 Å^{-1}). The background was described by a fourth-order polynomial. The fourth-order polynomial plus Gaussian peaks were fitted to the intensity data. Then, the background was subtracted, yielding the data points in the Figure. Subsequently, the positions of the five well-separated peaks labeled with bold-face Miller indices $\{h,k\} = \{0,1\}$; $\{1,1\}$; $\{2,0\}$; $\{2,1\}$; $\{4,3\}$ were refined by fitting, to the background subtracted data, five positions, five peak heights, and one common width of five Gaussian peaks. The resulting positions (diamonds in the inset which shows peak positions *versus* $\sqrt{h^2+hk+k^2}$) were then used to determine the lattice constant, $a = 61.3$ Å, by fitting them to a straight line through the origin according to equation (1). (The broken line in the inset corresponds to a lattice constant of $a = 62.5$ Å as determined by electron microscopy (Henderson *et al.*, 1990).) The positions of the remaining peaks were then fixed according to the $a = 61.3$ Å lattice constant (filled circles in the inset). Finally, the intensities of these remaining Bragg peaks were fitted. The sum of the fitted Gaussians is shown as a continuous line and the individual contributions are shown as broken lines. At the three positions marked with an asterisk, the peaks were found to have zero intensity.

deposited on 250 mM KCl and compressed to $\Pi = 10$ mN/m. The intensity was integrated over q_z in the range from 0 to 0.075 Å^{-1} and the background, described by a fourth-order polynomial, was subtracted. To test the assumption that the PM crystals at the air/water interface have hexagonal symmetry, we have plotted the scattering vector, q_{xy}, *versus* $\sqrt{h^2+hk+k^2}$ (inset in Figure 4) since for a 2D lattice with hexagonal symmetry, the quadratic form reads:

$$q_{xy}^{h,k} = \frac{4\pi}{a\sqrt{3}}\sqrt{h^2+hk+k^2} \qquad (1)$$

The plot reveals that the PM lattice has indeed hexagonal symmetry. The lattice constant a was evaluated by fitting a straight line to the data according to equation (1). For the data shown in Figure 4, the result is $a = 61.3(\pm 0.6)$Å. This value is significantly ($\sim 2\%$) smaller than the lattice constant determined with conventional diffraction methods on fully hydrated multilayer stacks for which $a = 62.5$ Å has been reported (Henderson *et al.*, 1986; Fitter *et al.*, 1998). For a more rigid membrane sample, obtained by partially delipidated purple membranes, we have observed a unit cell size of $a = 57.5$ Å, which is close to the value of $a = 56.9$ Å obtained from conventional X-ray diffraction on the delipidated PM patches (Fitter *et al.*, 1998).

Conclusions

By GIXD at small angles $2\theta_{xy}$ we have obtained a 2D powder diffraction pattern of a single layer of purple membrane, demonstrating the potential of this novel approach to structure determination of membrane-associated proteins. The data are qualitatively equivalent to the diffraction from multilamellar stacks of these lattices. In the future, efforts must be made into the following directions. (i) Methods should be developed for growing larger single 2D single crystals. For purple membrane, successful attempts at fusing individual smaller crystals to large single crystals with the help of detergents have been reported (Henderson *et al.*, 1990). (ii) The surface area which is illuminated by the X-ray beam should be as small as possible.

Together, these two developments would facilitate collecting better resolved 3D structural data, as diffraction experiments will be possible from one

2D single crystal within the protein monolayer. Reflections can be resolved which would overlap for a 2D crystal powder sample. Moreover, an improved signal-to-noise ratio will result from scattering from a single well-aligned sample.

The experiments reported here have demonstrated, as a first step using a single layer of purple membrane, the feasibility and advantages of the method. A sample of 10^{13} BR molecules in the beam are sufficient for a diffraction pattern (Figure 4), i.e. only 10^{-3} and 10^{-5} times the amount of the material required for conventional X-ray and neutron diffraction, respectively. Given adequate phases from electron microscopy, the projected structure of BR could, in principle, be calculated from these data.

Acknowledgments

We thank V. Hartmann for the AFM inspection of transferred PM. We are grateful to the HASYLAB at DESY, Hamburg, for beamtime at the intense beamline BW1 of the DORIS bypass (Frahm *et al*., 1995). This work was supported by the DFG (SFBs no. 189 to G.B., no. 294 to M.L. and no. 472 to N.A.D.), the BMBF (contract nos. 03-DE4DAR-1 and 03-LO4LEI-8), the Danish Dansync programme and the EC-TMR contract no. ERBFJ-GECT950059, as well as the Fonds der Chemischen Industrie (N.A.D. and M.L.). This research is part of the PhD theses of S.A.W.V. (Universität Düsseldorf) and of M.W. (Universität Leipzig).

An account of this study has been presented at the 2nd European Biophysics Congress, July 13-17, 1997, Orleans, France (Frenzen *et al*., 1997) and at the 42nd Annual Meeting of the Biophysical Society, February 22-26, 1998, Kansas City, USA (Verclas *et al*., 1998).

References

Als-Nielsen, J. & Kjaer, K. (1989). X-ray reflectivity and diffraction studies of lipid surfaces. In *Phase Transitions in Soft Condensed Matter* (Riste, T. & Sherrington, D., eds), vol. B211, pp. 113-138, Plenum Press, New York.

Als-Nielsen, J., Jacquemain, D., Kjaer, K., Lahav, M., Leveiller, F. & Leiserowitz, L. (1994). Principles and applications of grazing-incidence X-ray and neutron scattering from ordered molecular monolayers at the air-water interface. *Phys. Rep.* **246**, 251-313.

Bauer, P. J., Dencher, N. A. & Heyn, M. P. (1976). Evidence for chromophore-chromophore interactions in the purple membrane from reconstitution experiments of the chromophore-free membrane. *Biophys. Struct. Mech.* **2**, 79-92.

Darst, S. A., Ahlers, M., Meller, P. H., Kubalek, E. W., Blankenburg, R., Ribi, H. O., Ringsdorf, H. & Kornberg, R. D. (1991). Two-dimensional crystals of streptavidin on biotinylated lipid layers and their interaction with biotinylated macromolecules. *Biophys. J.* **59**, 387-396.

Dencher, N. A., Dresselhaus, D., Zaccai, G. & Büldt, G. (1989). Structural changes in bacteriorhodopsin during proton translocation revealed by neutron diffraction. *Proc. Natl Acad. Sci. USA*, **86**, 7876-7879.

Dencher, N. A., Heberle, J., Bark, K., Koch, M. H. J., Rapp, G., Oesterhelt, D., Bartels, K. & Büldt, G. (1991). Proton translocation and conformational changes during the bacteriorhodopsin photocycle: time-resolved studies with membrane-bound optical probes and X-ray diffraction. *Photochem. Photobiol.* **54**, 881-887.

Dietrich, C., Boscheinen, O., Scharf, K.-D., Schmitt, L. & Tempé, R. (1996). Functional immobilization of a DNA-binding protein at a membrane interface *via* histidine tag and synthetic chelator lipids. *Biochemistry*, **35**, 1100-1105.

Essen, L.-O., Siegert, R., Lehmann, W. D. & Oesterhelt, D. (1998). Lipid patches in membrane protein oligomers: crystal structure of the bacteriorhodopsin-lipid complex. *Proc. Natl Acad. Sci. USA*, **95**, 11673-11678.

Fitter, J., Lechner, R. E., Büldt, G. & Dencher, N. A. (1996). Temperature dependence of molecular motions in the membrane protein bacteriorhodopsin from QINS. *Physica, ser. B*, **226**, 61-65.

Fitter, J., Verclas, S. A. W., Lechner, R. E., Seelert, H. & Dencher, N. A. (1998). Function and pico-second dynamics of bacteriorhodopsin in purple membrane at different lipidation and hydration. *FEBS Letters*, **433**, 321-325.

Frahm, R., Weigelt, J., Meyer, G. & Materlik, G. (1995). X-ray undulator beamline BW1 at DORIS III. *Rev. Sci. Instrum.* **66**, 1677-1680.

Frenzen, A., Weygand, M., Verclas, S. A. W., Dencher, N. A., Büldt, G., Howes, P. B., Kjaer, K. & Lösche, M. (1997). Protein crystallography in 2D: grazing incidence X-ray diffraction from purple membrane patches at the air-water interface. *Eur. Biophys. J.* **26**, 116.

Furuno, T., Takimoto, K., Kouyama, T., Ikegami, A. & Sasabe, H. (1988). Photovoltaic properties of purple membrane Langmuir-Blodgett films. *Thin Solid Films*, **160**, 145-151.

Glaeser, R. M., Jubb, J. S. & Henderson, R. (1985). Structural comparison of native and deoxycholate-treated purple membrane. *Biophys. J.* **48**, 775-780.

Grigorieff, N., Ceska, T. A., Downing, K. H., Baldwin, J. M. & Henderson, R. (1996). Electron-crystallographic refinement of the structure of bacteriorhodopsin. *J. Mol. Biol.* **259**, 393-421.

Haas, H., Brezesinski, G. & Möhwald, H. (1995). X-ray diffraction of a protein crystal anchored at the air/water interface. *Biophys. J.* **68**, 312-314.

Henderson, R., Baldwin, J. M., Downing, K. H., Lepault, J. & Zemlin, F. (1986). Structure of purple membrane from *Halobacterium halobium*: recording, measurement and evaluation of electron micrographs at 3.5 Å resolution. *Ultramicroscopy*, **19**, 147-178.

Henderson, R., Baldwin, J. M., Ceska, T. A., Zemlin, F., Beckmann, E., Downing, K. H. & Lepault, J. (1990). Model for the structure of bacteriorhodopsin based on high-resolution electron cryomicroscopy. *J. Mol. Biol.* **213**, 899-929.

Hirata, Y. & Miyake, J. (1994). Molecular construction of a photosynthetic reaction center at the interface by its affinity with quinonylphospholipid. *Thin Solid Films*, **244**, 865-868.

Kjaer, K. (1994). Some simple ideas on X-ray reflection and grazing-incidence diffraction from thin surfactant films. *Physica, ser. B*, **198**, 100-109.

Koch, M. H. J., Dencher, N. A., Oesterhelt, D., Plöhn, H.-J., Rapp, G. & Büldt, G. (1991). Time-resolved

X-ray diffraction study of structural changes associated with the photocycle of bacteriorhodopsin. *EMBO J.* **10**, 521-526.

Krüger, P., Schalke, M., Wang, Z., Notter, R. H., Dluhy, R. A. & Lösche, M. (1999). Effect of hydrophobic surfactant proteins SP-B and SP-C on binary phospholipid monolayers. I. Fluorescence and dark-field microscopy. *Biophys. J.* In the press.

Lösche, M. & Möhwald, H. (1984). Fluorescence microscope to observe dynamical processes in monomolecular layers at the air/water interface. *Rev. Sci. Instrum.* **55**, 1968-1972.

Oesterhelt, D. & Stoeckenius, W. (1973). Functions of a new photoreceptor membrane. *Proc. Natl Acad. Sci. USA*, **70**, 2853-2857.

Pack, D. W., Chen, G. H., Maloney, K. M., Chen, C.-T. & Arnold, F. H. (1997). A metal-chelating lipid for 2D protein crystallization *via* coordination of surface histidines. *J. Am. Chem. Soc.* **119**, 2479-2487.

Pebay-Peyroula, E., Rummel, G., Rosenbusch, J. P. & Landau, E. M. (1997). X-ray structure of bacteriorhodopsin at 2.5 Ångstroms from microcrystals grown in lipidic cubic phases. *Science*, **277**, 1676-1681.

Ribi, H. O., Reichard, P. & Kornberg, R. D. (1987). Two-dimensional crystals of enzyme-effector complexes: ribonucleotide redustase at 18-Å resolution. *Biochemistry*, **26**, 7974-7979.

Schmitt, L. & Tempé, R. (1996). ATP-lipids - protein anchor and energy source in two dimensions. *J. Am. Chem. Soc.* **118**, 5532-5543.

Uzgiris, E. E. & Kornberg, R. D. (1983). Two-dimensional crystallization technique for imaging macromolecules, with an application to antigen-antibody-complement complexes. *Nature*, **301**, 125-129.

Verclas, S., Howes, P. B., Kjaer, K., Frenzen, A., Weygand, M., Büldt, G., Dencher, N. A. & Lösche, M. (1998). GIXD from purple membrane at the air/water interface. *Biophys. J.* **74**, A374.

Vineyard, G. H. (1982). Grazing-incidence diffraction and the distorted wave approximation for the study of surfaces. *Phys. Rev. ser. B*, **26**, 4146-4159.

Weissbuch, I., Popovitz-Biro, R., Lahav, M., Leiserowitz, L., Kjaer, K. & Als-Nielsen, J. (1997). Molecular self-assembly into crystals at air-liquid interfaces. In *Advances in Chemical Physics* (Prigogine, I. & Rice, S. A., eds), pp. 39-120, Wiley, New York.

Weygand, M., Wetzer, B., Pum, D., Sleytr, U. B., Cuvillier, N., Kjaer, K., Howes, P. B. & Lösche, M. (1999). Bacterial S-layer protein coupling to lipids. X-ray reflectivity and grazing incidence diffraction studies. *Biophys. J.* **76**, 458-468.

Edited by W. Baumeister

(Received 8 December 1998; received in revised form 12 February 1999; accepted 12 February 1999)